

PHYSICAL REVIEW C

NUCLEAR PHYSICS

THIRD SERIES, VOLUME 38, NUMBER 4

OCTOBER 1988

Multiconfiguration resonating-group study of scattering and reaction cross sections in the seven-nucleon system

Y. Fujiwara

Department of Physics, Kyoto University, Kyoto 606, Japan

Q. K. K. Liu

*Hahn-Meitner-Institut für Kernforschung, Berlin, Federal Republic of Germany
and School of Physics, University of Minnesota, Minneapolis, Minnesota 55455*

Y. C. Tang

School of Physics, University of Minnesota, Minneapolis, Minnesota 55455

(Received 29 April 1988)

Scattering and reaction cross sections in the seven-nucleon system are calculated in a multiconfiguration resonating-group study which consists of $t + {}^4\text{He}$, $n + {}^6\text{Li}$, and $n + {}^6\text{Li}^*$ cluster configurations. The results show that the diffraction and interference features of the experimental angular distributions can be well explained, but that the calculated magnitudes of the differential cross sections are generally too large. In addition, it is found that the calculated total reaction cross sections for the $t + {}^4\text{He}$ and $n + {}^6\text{Li}$ channels are only 30–40 % of the measured values, indicating that, for a satisfactory explanation of all the important features of the seven-nucleon system, more cluster configurations must still be incorporated into the resonating-group formulation.

I. INTRODUCTION

In a recent investigation,¹ we have studied the properties of the seven-nucleon system by performing a multiconfiguration resonating-group calculation in which the $t + {}^4\text{He}$, $n + {}^6\text{Li}$, and $n + {}^6\text{Li}^*$ cluster configurations are included. To ensure the reliability of the result, we have made careful choices of internal wave functions which account for cluster correlations, satisfy the variational stability conditions, and explain the form-factor data over a large range of q^2 . The calculation was carried out with a central nucleon-nucleon potential containing a soft repulsive core, and the result shows that the calculated level spectrum agrees quite well with the level spectrum empirically determined and useful information concerning the effects of specific distortion and nucleon exchanges can be obtained.

The investigation, reported in Ref. 1, was concentrated on studying the dependence of the S -matrix elements on the extension of the model space employed in the calculation. Here we shall continue the study by examining the behavior of the scattering and reaction cross sections in the higher excitation-energy region where sharp resonances of the compound nucleus no longer exist. Additionally, we shall, of course, also compare calculated and

experimental results in order to see how well our multiconfiguration study can explain the essential characteristics of the measured cross-section angular distributions in the seven-nucleon system.

It should be mentioned that a similar multiconfiguration study has also been carried out by Hofmann *et al.*² The conclusions reached there agree generally with those obtained in our investigation. Similar to our study reported in Ref. 1, the main emphasis of these authors was also on the examination of the behavior of the S -matrix elements. Because of the limitation imposed by their consideration of a rather small number of partial waves in various channels, they have not attempted to calculate differential scattering and reaction cross sections in the higher-energy region.

The outline of this paper is as follows. In the next section, a very brief description of the formulation of the seven-nucleon multiconfiguration study is presented. The dependence of the calculated differential scattering and reaction cross sections on the extension of the model space is then discussed in Sec. III. In Sec. IV, we compare the calculated and experimental results for the various cross-section angular distributions. Finally, in Sec. V, we discuss the findings of this investigation and make some concluding remarks.

II. BRIEF DESCRIPTION OF THE FORMULATION

The formulation of the seven-nucleon problem with multiple cluster configurations is given in Ref. 1 and, hence, will not be further described here. It suffices to mention that the two-cluster configurations included in the calculation are the $t + {}^4\text{He}$, $n + {}^6\text{Li}$, and $n + {}^6\text{Li}^*$ configurations, with ${}^6\text{Li}^*$ being the $T=0$ excited state of ${}^6\text{Li}$ having a $d + \alpha$ cluster structure with relative orbital angular momentum $I=2$. In addition, the $d + {}^5\text{He}$ configuration has also been included to expand the model space; however, because of computational limitation, its consideration was only made in the state with total orbital angular momentum L equal to 1, where this particular cluster configuration is expected to contribute most significantly.

The nucleon-nucleon potential used is purely central with a Serber exchange mixture. For simplicity in calculation and interpretation, noncentral and Coulomb effects are not considered. This is not a serious defect since, at the relatively high energies to be studied here, these effects have rather minor consequences on the cross-section results and are not essential for an understanding of the basic behavior of the intricate interplay among various cluster configurations.

One important feature of this multiconfiguration study should be emphasized. To make certain that the results obtained should be reliable, we have taken precaution to choose cluster internal wave functions³ which meet certain important criteria. These criteria involve careful considerations of the nucleon-correlation structure, the form-factor behavior, and the variational stability condition.

The calculations are performed in a number of model spaces which are defined as follows: (i) single configuration SC1 space with only the $t + {}^4\text{He}$ cluster configuration, (ii) single-configuration SC2 space with only the $n + {}^6\text{Li}$ cluster configuration, (iii) double-configuration DC space consisting of both the $t + {}^4\text{He}$ and the $n + {}^6\text{Li}$ configurations, and (iv) triple-configuration TC space which is spanned by not only the $t + {}^4\text{He}$ and the $n + {}^6\text{Li}$ configurations, but also the $n + {}^6\text{Li}^*$ configuration. The influence of the $d + {}^5\text{He}$ configuration will also be examined, but, as has been mentioned previously, only in the $L = 1$ state.

Using the calculated S -matrix elements from Ref. 1, one can easily compute the scattering and reaction cross sections in a state of definite total spin angular momentum S ($S = \frac{1}{2}$ or $\frac{3}{2}$). The differential scattering cross section in channel i ($i = 1$ or 2 , with channels 1 and 2 being the $t + {}^4\text{He}$ and $n + {}^6\text{Li}$ channels, respectively) is given by

$$\sigma(\theta) = |A_{ii}|^2, \quad (1)$$

with

$$A_{ii} = \sum_{L=0}^{\infty} \frac{2L+1}{2ik_i} (S_{ii}^L - 1) P_L(\cos\theta). \quad (2)$$

Similarly, the differential reaction cross section leading from channel i to channel f is given by

$$\sigma(\theta) = |A_{fi}|^2, \quad (3)$$

with

$$A_{fi} = \sum_{L=0}^{\infty} \frac{2L+1}{2ik_i} S_{fi}^L P_L(\cos\theta). \quad (4)$$

Also, the total reaction cross section from channel i to channel f can be calculated by using the equation

$$\sigma_R = \sum_{L=0}^{\infty} \frac{\pi}{k_i^2} (2L+1) (\eta_{fi}^L)^2, \quad (5)$$

with $\eta_{fi}^L = |S_{fi}^L|$ being the transmission coefficient. In the above equations, the quantities k_1 and k_2 are asymptotic wave numbers which are related through the equation

$$E_1 = E_2 + E_{\text{th}}, \quad (6)$$

where E_{th} , equal to 3.15 MeV, is the calculated $n + {}^6\text{Li}$ threshold energy with respect to the $t + {}^4\text{He}$ channel, and E_1 and E_2 denote, respectively, the relative energies in the c.m. system of the t and ${}^4\text{He}$ clusters in channel 1 and of the neutron and the ${}^6\text{Li}$ cluster in channel 2.

III. SCATTERING AND REACTION CROSS SECTIONS IN VARIOUS MODEL SPACES

As was discussed in Ref. 1, the TC calculation yields a number of ${}^7\text{Li}$ resonance levels in the energy region where E_1 is smaller than about 12 MeV. In Fig. 1, we show the effects of these levels on the calculated total cross sections σ_R and σ_R^* for the ${}^4\text{He}(t,n){}^6\text{Li}$ and ${}^4\text{He}(t,n){}^6\text{Li}^*$ reactions, respectively. From this figure, one notes that, for $E_1 \lesssim 12$ MeV, σ_R does have an appreciable and oscillatory energy dependence. Since it is to be expected that the S -matrix element will change substantially with the extension of the model space in the region where relatively sharp resonance levels exist and that even a rather extensive multiconfiguration study of the type employed here will not precisely yield the positions and widths of the compound-nucleus resonances, it seems prudent that one should appropriately avoid the low-energy region in a cross-section study and examine the results only at energies with E_1 larger than about 12 MeV.

The importance of the $n + {}^6\text{Li}^*$ configuration is demonstrated also in Fig. 1. Here one sees that, for E_1 higher than about 10 MeV, σ_R^* has an appreciably larger magnitude than σ_R (see also Ref. 2). At $E_1 = 15.95$ MeV, σ_R and σ_R^* are equal to 34 and 102 mb, respectively, which are consistent with the measured values⁴ of 32 ± 1 and 81 ± 2 mb for the ${}^4\text{He}({}^3\text{He}, p)$ reactions leading to the ground and first excited states of ${}^6\text{Li}$. On the other hand, the calculated total reaction cross section for the $t + {}^4\text{He}$ channel at this energy is 136 mb, which is only about 30% of the measured value⁴ of 433 ± 10 mb for the ${}^3\text{He} + {}^4\text{He}$ channel. This indicates that even more cluster configurations must still be incorporated into the

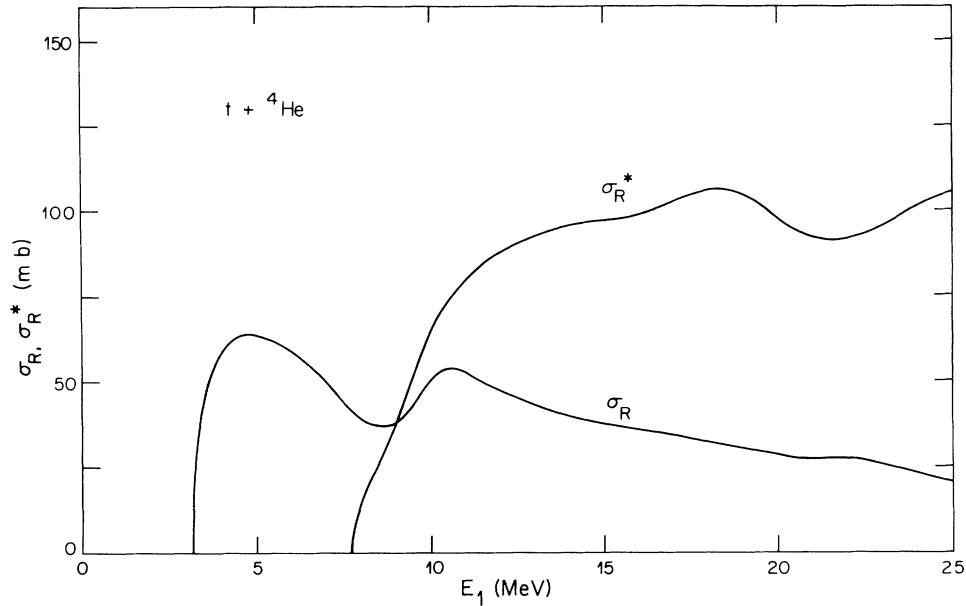


FIG. 1. Calculated cross sections σ_R and σ_R^* for the ${}^4\text{He}(t,n){}^6\text{Li}$ and ${}^4\text{He}(t,n){}^6\text{Li}^*$ reactions, respectively.

seven-nucleon calculation. Quite obviously, such an improvement may escalate the computational complexity to an impractical extent; however, from a microscopic viewpoint, this may be unavoidable if one desires to explain all the important features of this complicated many-nucleon system.

Next, the dependence of the calculated differential cross sections on the extension of the model space is stud-

ied. In Figs. 2–4, we show, respectively, the cross sections for $t + {}^4\text{He}$ scattering at $E_1 = 20$ MeV calculated in the SC1 (dashed curve) and TC (solid curve) spaces, for $n + {}^6\text{Li}$ scattering at $E_2 = 20$ MeV calculated in the SC2 (dashed curve) and TC (solid curve) spaces, and for the ${}^4\text{He}(t,n){}^6\text{Li}$ reaction at $E_1 = 20$ MeV calculated in the DC (dashed curve) and TC (solid curve) spaces. Here one notes a striking feature; i.e., as the model space is expand-

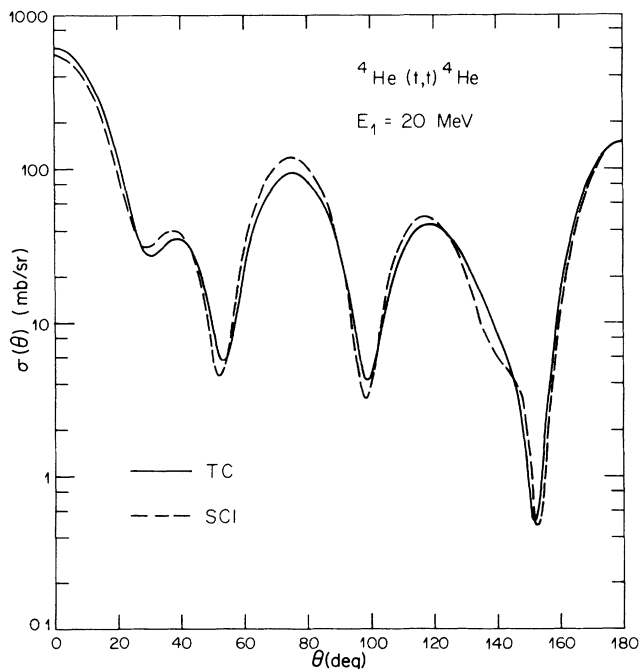


FIG. 2. Comparison of $t + {}^4\text{He}$ differential cross sections at $E_1 = 20$ MeV, obtained with SC1 (dashed curve) and TC (solid curve) calculations.

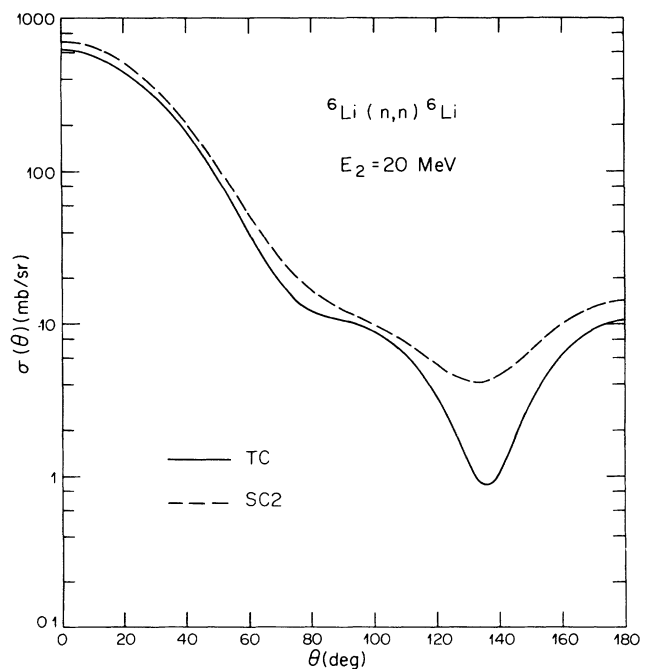


FIG. 3. Comparison of $n + {}^6\text{Li}$ differential cross sections at $E_2 = 20$ MeV, obtained with SC2 (dashed curve) and TC (solid curve) calculations.

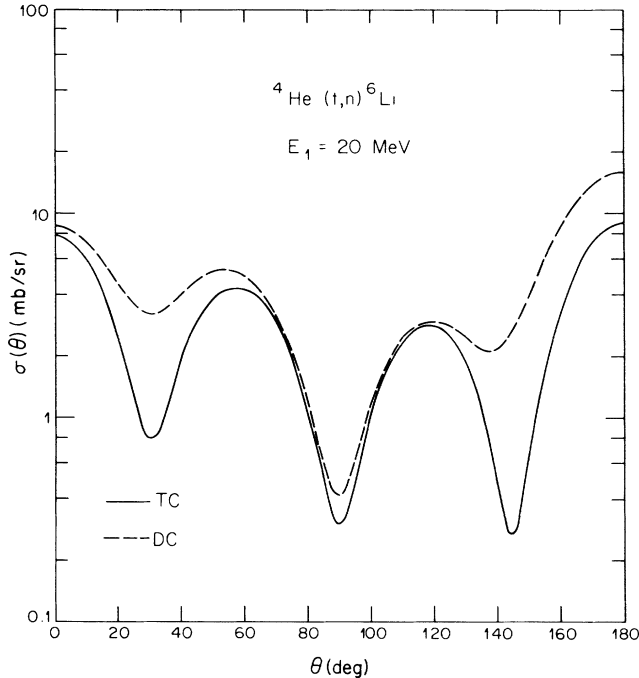


FIG. 4. Comparison of differential cross sections for the ${}^4\text{He}(t,n){}^6\text{Li}$ reaction at $E_1 = 20$ MeV, obtained with DC (dashed curve) and TC (solid curve) calculations.

ed, the essential characteristics of the angular distributions do not seem to change appreciably. From these figures, one finds not only that the angular positions of the peaks and valleys remain essentially the same, but also that the relative magnitudes of the peaks are similar. It turns out that an enlargement of the model space serves mainly to lower the general magnitudes of the calculated cross sections (see especially Figs. 3 and 4). This is certainly an interesting and useful finding, since it suggests that, at least in light systems and at relatively high energies, one can hope to explain the diffraction and interference features exhibited in cross-section angular distributions by performing only comparatively simple calculations in rather restricted model spaces.

The effect of further enlarging the model space by adding onto the TC calculation the $d + {}^5\text{He}$ cluster configuration (i.e., the QC calculation) has also been briefly examined in the $L = 1$ state. The results at $E_1 = 20$ MeV show that, in going from the TC to the QC case, the total reaction cross section in this angular-momentum state for the $t + {}^4\text{He}$ channel increases from 10.8 to 15.0 mb, while the cross section for the ${}^4\text{He}(t,n){}^6\text{Li}$ reaction decreases from 7.1 to 3.7 mb. Both of these results are rather expected, and are consistent with the interpretation that the addition of the $d + {}^5\text{He}$ channel has the main effect of simply draining off flux from the $t + {}^4\text{He}$ channel and, thus, leaves a smaller fraction of the incident flux to initiate the ${}^4\text{He}(t,n){}^6\text{Li}$ reaction.

IV. COMPARISON WITH EXPERIMENT

In this section, we compare the cross sections calculated in the TC model space with experimental values. Based on the discussion given in the preceding section, it is reasonable to anticipate that the calculated results will yield quite correctly the oscillatory features of the measured angular distributions, but that the magnitudes of the calculated cross sections will generally be too large.

That the above anticipation turns out to be indeed true can be seen from Figs. 5 and 6, where we compare the calculated and experimental^{5,6} results for ${}^3\text{He} + {}^4\text{He}$ scattering at E_1 equal to 15.95 and 24.36 MeV, respectively. Here one sees that, except at small forward angles where our omission of Coulomb effects causes a predictable underestimate in the cross-section values, the calculated curve reproduces not only the angular positions of the peaks and valleys, but also all the detailed structure of the angular distributions. The discrepancy between calculated and experimental magnitudes is larger at 24.36 MeV than at 15.95 MeV. This may be correlated with the fact that, in a calculation⁷ where a phenomenological imaginary potential is employed to crudely account for reaction effects in the ${}^3\text{He} + {}^4\text{He}$ system, the resultant reaction cross section at 24.36 MeV turns out to be also appreciably larger than that at 15.95 MeV.

The situation for $n + {}^6\text{Li}$ scattering and ${}^6\text{Li}(p, {}^3\text{He}){}^4\text{He}$ reaction is similar. In Figs. 7 and 8, we compare, respec-

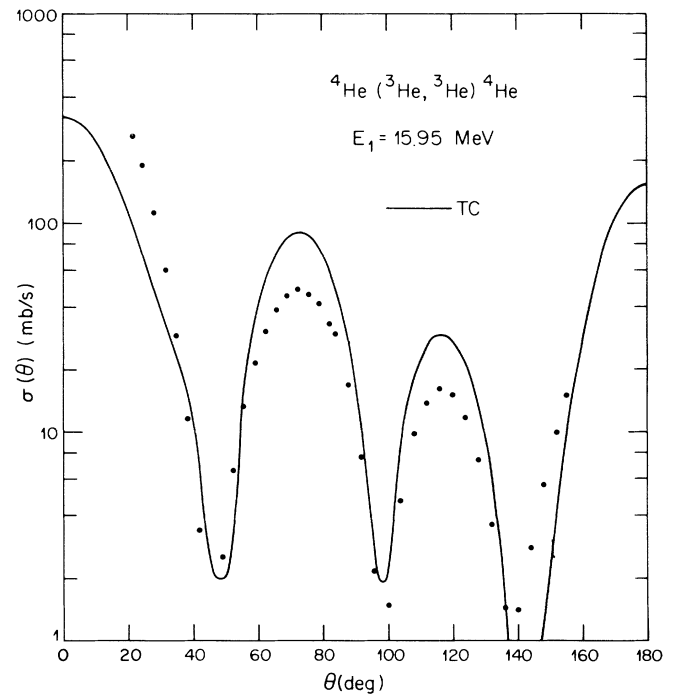


FIG. 5. Comparison of differential cross sections for $t + {}^4\text{He}$ scattering at $E_1 = 15.95$ MeV calculated in the TC model space with experimental results. Experimental data shown are those of Ref. 5.

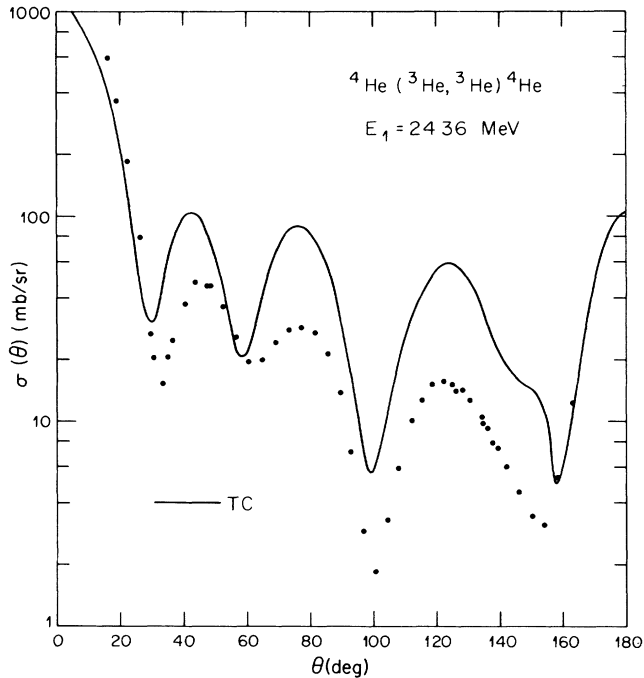


FIG. 6. Comparison of differential cross sections for $t + {}^4\text{He}$ scattering at $E_1 = 24.36$ MeV calculated in the TC model space with experimental results. Experimental data shown are those of Ref. 6.

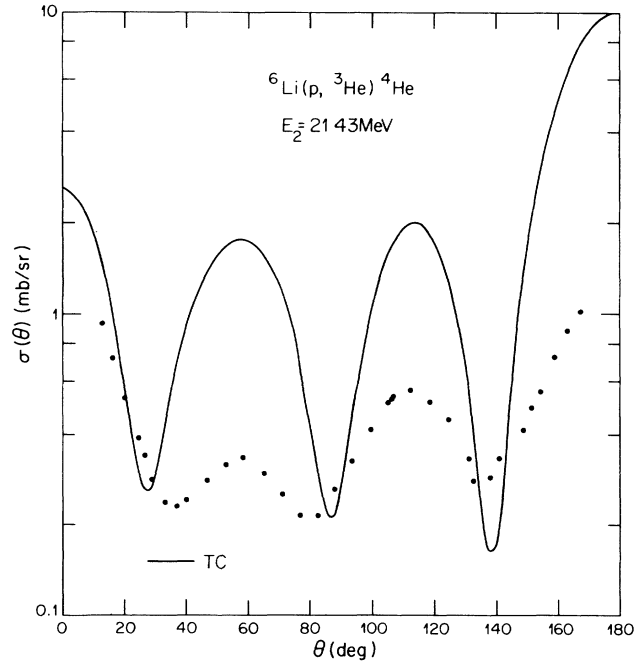


FIG. 8. Comparison of differential cross sections for ${}^6\text{Li}(p, {}^3\text{He}){}^4\text{He}$ reaction at $E_2 = 21.43$ MeV calculated in the TC model space with experimental results. Experimental data shown are those of Ref. 9.

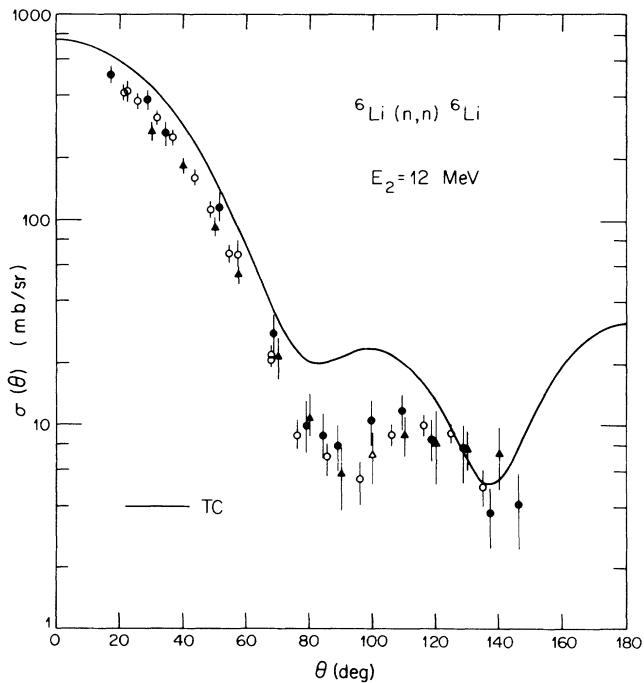


FIG. 7. Comparison of differential cross sections for $n + {}^6\text{Li}$ scattering at $E_2 = 12$ MeV calculated in the TC model space with experimental results. Experimental data shown are those of Ref. 8.

tively, the calculated and experimental^{8,9} cross sections for $n + {}^6\text{Li}$ scattering at $E_2 = 12$ MeV and for ${}^6\text{Li}(p, {}^3\text{He}){}^4\text{He}$ reaction at $E_2 = 21.43$ MeV. From these figures, one finds again that the main discrepancy is only in the magnitudes of the cross sections. In the case of $n + {}^6\text{Li}$ scattering, the calculated minimum at about 140° is too deep (relative to the maximum at about 100°), which is clearly due to the omission of noncentral effects in our investigation. The calculated total reaction cross section for the $n + {}^6\text{Li}$ channel is 276 mb. This cannot be compared with experiment at the present moment, since no measurement has yet been made at this energy. However, at a neighboring energy of 8.57 MeV, the experimental value¹⁰ is known to be about 650 mb, indicating that our calculation yields only about 40% of the total reaction cross section. Therefore, this explains nicely the overestimate of the cross-section values in our study and points again to the fact that more cluster configurations are needed in our calculation for a satisfactory explanation of all the important features in the seven-nucleon system.

V. CONCLUSION

In this investigation, we examine the behavior of the differential scattering and reaction cross sections in the seven-nucleon system using a multiconfiguration resonating-group study which consists of $t + {}^4\text{He}$, $n + {}^6\text{Li}$, and $n + {}^6\text{Li}^*$ cluster configurations. By studying the dependence of these cross sections on the extension of the model space and by comparing calculated and experimen-

tal results, we obtain the interesting finding that, at relatively high energies where sharp resonances of the compound nucleus do not exist, the essential characteristics of the oscillatory patterns exhibited in cross-section angular distributions can already be explained by carrying out comparatively simple resonating-group calculations in rather restricted model spaces.

There is indication, however, that our present calculation is not extensive enough. In contrast to the above-mentioned finding, our study also shows that the calculated total reaction cross sections for the $t + {}^4\text{He}$ and $n + {}^6\text{Li}$ channels are too small and that the calculated differential cross sections for ${}^3\text{He} + {}^4\text{He}$ and $n + {}^6\text{Li}$ scattering and ${}^6\text{Li}(p, {}^3\text{He}){}^4\text{He}$ reaction have magnitudes which are generally larger than the magnitudes experimentally determined. This suggests that, for a detailed understanding of all the important features in this many-nucleon system, more cluster configurations must still be incorporated into the resonating-group calculation. Based on the experience gained from a recent four-nucleon investigation,¹¹ our opinion is that, in addition to the $t + {}^4\text{He}$, $n + {}^6\text{Li}$, and $n + {}^6\text{Li}^*$ configurations employed here, it would be necessary to further include the $d + {}^5\text{He}$ configuration and many pseudoinelastic configurations¹² which involve pseudoexcited states of the clusters d , t , ${}^5\text{He}$, ${}^6\text{Li}$, and ${}^6\text{Li}^*$. The inclusion of these pseudoinelastic

channels is important in order to adequately take into account the ${}^4\text{He} + d + n$ and ${}^4\text{He} + n + n + p$ reaction channels which are already open in the low-excitation region. On the other hand, cluster configurations such as $p + {}^6\text{He}$ and $n + {}^6\text{Li}(T=1)$ may have only minor influence, since it has been experimentally found⁴ that the cross section for the ${}^4\text{He}({}^3\text{He}, p)$ reaction leading to the $T=1$ state of ${}^6\text{Li}$ at 3.56 MeV is very small.

A resonating-group calculation containing all the important cluster configurations mentioned above would be a formidable task and may not even be practicable at the present moment. As a preliminary step, one may wish to simply add phenomenological imaginary potentials into the present formulation. Such a procedure is, of course, rather undesirable from a microscopic standpoint; however, in view of the experience obtained here and in the five-nucleon case carried out previously,¹³ we feel that it may very well yield reasonable results in comparison with experiment and, thereby, shed some light upon the reaction mechanisms in the seven-nucleon system.

This research was supported in part by the US Department of Energy under Contract No. DOE/DE-AC02-79-ER-10364 and by the Supercomputer Institute at the University of Minnesota.

¹Y. Fujiwara and Y. C. Tang, Phys. Rev. C **31**, 342 (1985).

²H. M. Hofmann, T. Mertelmeier, and W. Zahn, Nucl. Phys. **A410**, 208 (1983).

³Y. Fujiwara and Y. C. Tang, Phys. Rev. C **27**, 2457 (1983).

⁴J. A. Koepke and R. E. Brown, Phys. Rev. C **16**, 18 (1977).

⁵C. G. Jacobs, Jr. and R. E. Brown, Phys. Rev. C **1**, 1615 (1970).

⁶P. Schwandt, B. W. Ridley, S. Hayakawa, L. Put, and J. J. Kraushaar, Phys. Lett. **30B**, 30 (1969).

⁷J. A. Koepke, R. E. Brown, Y. C. Tang, and D. R. Thompson, Phys. Rev. C **9**, 823 (1974).

⁸D. I. Garber, L. G. Strömberg, M. D. Goldberg, D. E. Cullen, and V. M. May, Brookhaven National Laboratory Report No. 400, 1970; V. Abbondanno, R. Giacomich, L. Granata,

M. Lagonegro, and G. Poiani, Nuovo Cimento **66A**, 139 (1970).

⁹K. Schenk, M. Mörike, G. Staudt, P. Turek, and D. Clement, Phys. Lett. **52B**, 36 (1974).

¹⁰J. A. Cookson, D. Dandy, and J. C. Hopkins, Nucl. Phys. **A91**, 273 (1967).

¹¹H. Kanada, T. Kaneko, and Y. C. Tang, Phys. Rev. C **34**, 22 (1986).

¹²H. Kanada, T. Kaneko, P. N. Shen, and Y. C. Tang, Nucl. Phys. **A457**, 93 (1986).

¹³F. S. Chwieroth, Y. C. Tang, and D. R. Thompson, Phys. Rev. C **9**, 56 (1974).